Diversity and PAPR Enhancement in OTFS using Indexing

Jickson K Francis, Rose Mary Augustine, and A. Chockalingam
Department of ECE, Indian Institute of Science, Bangalore 560012

***Abstract*—In this paper, we investigate indexing of delay-Doppler (DD) bins in orthogonal time frequency space (OTFS) modulation and propose indexing designs that enhance the diversity order of OTFS. It has been shown in the literature that the asymptotic diversity order of conventional OTFS (without indexing) is just one. In this paper, we show that indexing in the DD domain in OTFS can be used to enhance the asymptotic diversity order to two. Towards this, we consider 2-dimension indexing in OTFS, where indexing is done along both delay as well as Doppler axes. We achieve the enhanced diversity order of two by proposing indexing designs that provably eliminate all the rank one difference matrices. Our simulation results also validate this analytically proven diversity order of two in indexed OTFS. In addition, indexing is shown to offer improved PAPR (peak-to-average power ratio) performance of OTFS.**

Keywords: OTFS modulation, delay-Doppler domain, indexing, diversity, PAPR.

I. Introduction

Orthogonal time frequency space (OTFS) modulation is a promising modulation technique proposed recently in [1]. It multiplexes information symbols over bins in the delay-Doppler (DD) grid. The well known orthogonal frequency division multiplexing (OFDM) technique multiplexes the information symbols over bins in the frequency axis (which is the inverse of the delay axis), and a 1-dimensional transform (inverse fast Fourier transform) maps the symbols to time domain for transmission on the channel. OTFS, on the other hand, first uses a 2-dimensional transform (inverse simplectic finite Fourier transform) that transforms the symbols from DD grid to time-frequency (TF) grid. A second 2-dimensional transform (Heisenberg transform) further transforms the symbols from TF domain to time domain for transmission [1]- [4]. Several studies in the literature have reported superior performance of OTFS compared to OFDM, generalized frequency division multiplexing (GFDM), and single-carrier FDMA (SC-FDMA) [1]- [7], particularly in high-mobility/high-Doppler environments, making OTFS attractive for use cases such as V2X, high-speed train, and mmWave communications. In addition to superior performance in high-mobility channels, OTFS has also been shown to achieve superior performance in static multipath channels as well, owing to the structural equivalence between OTFS and asymmetric OFDM (A-OFDM) [8], [9], suggesting the suitability of OTFS for a range of mobility scenarios (from no-mobility to high-mobility scenarios).

Conveying information bits through indexing of transmission entities, such as transmit antennas, subcarriers, time slots, precoders, popularly known in the literature as index modulation, is known to offer attractive benefits such as good performance and hardware simplicity [10]- [12]. In index modulation, the choice of transmission entities to be activated in a given channel use conveys additional information bits. Conveying bits through indexing has several advantages, e.g., i) the choose operation can lead to higher rates compared to conventional modulation, and ii) to achieve a certain rate (in bits per channel use), the size of the conventional modulation alphabet used can be reduced and this can lead to improved bit error performance. Performance of indexing in OTFS, obtained through simulations, has been reported recently in [13]. But this work does not provide a formal analytical treatment of the diversity performance achieved by indexed OTFS. Also, PAPR performance of indexed OTFS is not addressed. Our work in this paper addresses these two aspects of indexed OTFS. In this context, we note that it has been shown in the literature that the asymptotic diversity order of conventional OTFS (without indexing) is just one [6]. Our new contribution in this paper shows that indexing in the DD domain in OTFS can be used to enhance the asymptotic diversity order to two. Towards this, we consider 2-dimension (2D) indexing in OTFS, where indexing is done along both delay as well as Doppler axes. We achieve the enhanced diversity order of two by proposing indexing designs that provably eliminate all the rank one difference matrices. Our simulation results also validate this analytically proven diversity order of two in indexed OTFS. Further, we investigate the effect of indexing on the PAPR performance of OTFS and show that improved PAPR performance of OTFS is achieved using Doppler indexing.

The rest of the paper is organized as follows. The system model and 2D indexing in OTFS are presented in Sec. II. Indexing designs for second order diversity and proof are presented in Sec. III. Diversity and PAPR results are presented in IV. Conclusions are presented in Sec. V.

II. 2-Dimension Indexing in OTFS

OTFS is a 2D modulation technique which uses the DD grid to multiplex information symbols. The $N \times M$ DD grid is a collection of DD bins, given by

$$\{(\tfrac{k}{NT}, \tfrac{l}{M\Delta f}), k = 0, 1, \cdots, N-1, l = 0, 1, \cdots, M-1\}. \quad (1)$$

where M and N are the number of delay and Doppler bins, respectively, and $\frac{1}{M\Delta f}$ and $\frac{1}{NT}$ are the delay and Doppler resolutions, respectively. Let $x[k, l]$ denote the information symbol from a complex modulation alphabet $\mathcal{A}$ in the (k, l)th DD bin. The information symbol $x[k, l]$ in the DD domain is transformed to TF domain by using inverse simplectic finite

This work was supported in part by the J. C. Bose National Fellowship, Department of Science and Technology, Government of India. Rose Mary Augustine is with Defense Avionics Research Establishment (DARE), DRDO, Bangalore.

Fourier transform (ISFFT). The TF domain signal corresponding to $x[k,l]$ is given by

$$X[n,m] = \frac{1}{MN}\sum_{k=0}^{N-1}\sum_{l=0}^{M-1} x[k,l]e^{j2\pi(\frac{nk}{N}-\frac{ml}{M})}. \quad (2)$$

The TF domain signal is transmitted as a packet burst which has a duration of NT and occupies a bandwidth $B = \frac{M}{T} = M\Delta f$. The TF domain signal is converted into the time domain by using Heisenberg transform, as

$$x(t) = \sum_{n=0}^{N-1}\sum_{m=0}^{M-1} X[n,m]g_{tx}(t-nT)e^{j2\pi m\Delta f(t-nT)}. \quad (3)$$

Here, $g_{tx}(t)$ denotes the transmit pulse shape. The transmitted signal $x(t)$ passes through the channel and the received time domain signal $y(t)$ is matched filtered with a receive pulse $g_{rx}(t)$. This gives the cross-ambiguity function, given by $A_{g_{rx},y}(\tau,\nu) = \int g^*_{rx}(t-\tau)y(t)e^{-j2\pi\nu(t-\tau)}\mathrm{d}t$. We assume the pulses $g_{rx}(t)$ and $g_{tx}(t)$ to satisfy the biorthogonality condition. The $A_{g_{rx},y}(\tau,\nu)$ is sampled at $\tau = nT$ and $\nu = m\Delta f$ to get the TF domain signal, as $Y[n,m] = A_{g_{rx},y}(\tau,\nu)|_{\tau=nT,\nu=m\Delta f}$. The above TF domain signal is converted to DD domain by using simplectic finite Fourier transform (SFFT), as

$$y[k,l] = \sum_{n=0}^{N-1}\sum_{m=0}^{M-1} Y[n,m]e^{-j2\pi(\frac{nk}{N}-\frac{ml}{M})}. \quad (4)$$

Consider a channel with P taps from P clusters of reflectors, each associated with a delay τ_i, a Doppler ν_i, and a complex fade coefficient h_i. This channel in DD domain can be written as $h(\tau,\nu) = \sum_{i=1}^{P} h_i\delta(\tau-\tau_i)\delta(\nu-\nu_i)$. Letting $\tau_i \triangleq \frac{\alpha_i}{M\Delta f}$ and $\nu_i \triangleq \frac{\beta_i}{NT}$, where α_i and β_i are integers, the input-output relation of the P tap channel is given by

$$y[k,l] = \sum_{i=1}^{P} h'_i x[(k-\beta_i)_N,(l-\alpha_i)_M] + v[k,l], \quad (5)$$

where $v[k,l]$ denotes AWGN and $h'_i = h_i e^{-j2\pi\nu_i\tau_i}$. The h_is are assumed to be i.i.d and distributed as $\mathcal{CN}(0,1/P)$, assuming uniform scattering profile. The input-output equation in (5) can be represented in vector form as [5]

$$\mathbf{y} = \mathbf{H}\mathbf{x} + \mathbf{v}, \quad (6)$$

where $\mathbf{H} \in \mathbb{C}^{MN\times MN}$ and $\mathbf{x},\mathbf{y},\mathbf{v} \in \mathbb{C}^{MN\times 1}$. The elements of $\mathbf{x},\mathbf{y}$ and $\mathbf{v}$ are given by $x_{k+Nl} = x[k,l]$, $y_{k+Nl} = y[k,l]$, and $v_{k+Nl} = v[k,l]$, respectively, with $k = 0,\cdots,N-1$, $l = 0,\cdots,M-1$. The matrix $\mathbf{H}$ in (6) is a block circulant matrix with circulant blocks of size $MN\times MN$, with each row having P non-zero elements.

A. 2D indexing in OTFS

In this subsection, we introduce indexing schemes which use both delay and Doppler axis for indexing. Depending upon how the delay and Doppler bins are selected for activation in an $N\times M$ DD grid, three types of 2D indexing are as follows.

1) Type 1: This type of indexing involves two steps of selection of active DD bins. First, K_2 active Doppler indices out of N available Doppler indices are selected, i.e., select K_2 rows in the $N\times M$ DD grid. This results in $\binom{N}{K_2}$ possible combination of active Doppler indices, and $\left\lfloor \log_2\binom{N}{K_2}\right\rfloor$ information bits are used for this selection operation. Next, for each of the Doppler indices selected in the first step, K_1 active delay indices out of M available delay indices are selected, which is done using $K_2\left\lfloor \log_2\binom{M}{K_1}\right\rfloor$ information bits. From the above two steps, there are K_1K_2 active DD bins out of MN bins in the $N\times M$ DD grid. In each of these active bins, a symbol from a modulation alphabet $\mathcal{A}$ is multiplexed, i.e., $K_1K_2\log_2|\mathcal{A}|$ bits are multiplexed in the K_1K_2 active bins. So, the achieved rate in Type 1 indexing is given by

$$\eta_{\text{type1}} = \frac{1}{MN}\Bigg(\left\lfloor \log_2\binom{N}{K_2}\right\rfloor + K_2\left\lfloor \log_2\binom{M}{K_1}\right\rfloor + K_1K_2\log_2|\mathcal{A}|\Bigg) \quad \text{bpcu}. \quad (7)$$

It is noted that 1D indexing along the delay axis is a special case of Type 1 indexing with $K_2 = N$.

2) Type 2: Type 2 indexing is similar to Type 1 indexing except the order of selection of delay and Doppler indices are reversed. Here, K_1 out of M delay indices are selected in the first step, followed by selection of K_2 out of N Doppler indices in the second step for each of the selected delay indices, and K_1K_2 modulation symbols are multiplexed on the selected bins. The achieved rate in Type 2 indexing is

$$\eta_{\text{type2}} = \frac{1}{MN}\Bigg(\left\lfloor \log_2\binom{M}{K_1}\right\rfloor + K_1\left\lfloor \log_2\binom{N}{K_2}\right\rfloor + K_1K_2\log_2|\mathcal{A}|\Bigg) \quad \text{bpcu}. \quad (8)$$

It can be observed that 1D indexing along the Doppler axis is a special case of Type 2 indexing with $K_1 = M$.

3) Type 3: Here, K_1 out of M delay indices and K_2 out of N Doppler indices are selected simultaneously using a total of $\left\lfloor \log_2\binom{M}{K_1}\right\rfloor + \left\lfloor \log_2\binom{N}{K_2}\right\rfloor$ information bits. Information symbols are multiplexed on the resulting K_1K_2 active bins, leading to an achieved rate of

$$\eta_{\text{type3}} = \frac{1}{MN}\Bigg(\left\lfloor \log_2\binom{M}{K_1}\right\rfloor + \left\lfloor \log_2\binom{N}{K_2}\right\rfloor + K_1K_2\log_2|\mathcal{A}|\Bigg) \quad \text{bpcu}. \quad (9)$$

Figure 1 shows examples of DD grids with active (black) and inactive (white) bins for each type of 2D indexing for $M = 8$, $N = 6$, $K_1 = 5$, and $K_2 = 4$.

III. Indexing designs for second order diversity

In this section, we analyze the asymptotic diversity order of indexed OTFS and obtain indexing designs that achieve second order diversity. Towards this, we consider the following alternate form of the vectorized input-output relation in (6):

$$\mathbf{y}^T = \mathbf{h}'\mathbf{X} + \mathbf{v}^T. \quad (10)$$

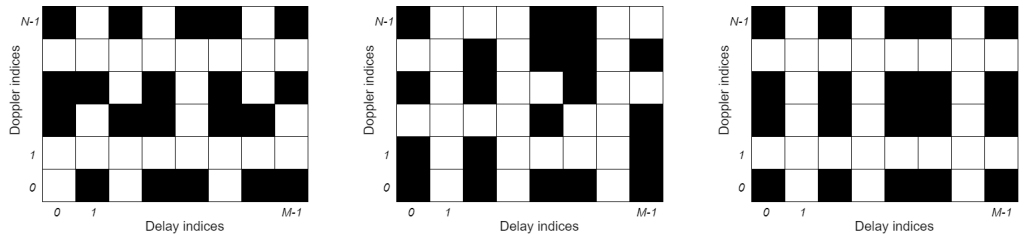

(a) Type 1 indexing (b) Type 2 indexing (c) Type 3 indexing

Fig. 1. 2-Dimensional indexing in $N \times M$ DD grid for $M = 8,\ N = 6,\ K_1 = 5,\ K_2 = 4$. Black bins: active. White bins: inactive.

In (10), $\mathbf{y}^T$ is the $1 \times MN$ received vector, $\mathbf{h}'$ is a $1 \times P$ vector, ith element of $\mathbf{h}'$ is $h'_i = h_i e^{-j2\pi\nu_i\tau_i}$, and $\mathbf{X}$ is $P \times MN$ matrix whose $(k+Nl)$th column, represented by $\mathbf{X}[k+Nl], k = 0, 1, \cdots, N-1, l = 0, 1, \cdots, M-1$, is given by

$$\mathbf{X}[k+Nl] = \begin{bmatrix} x_{(k-\beta_1)_N+N(l-\alpha_1)_M} \\ x_{(k-\beta_2)_N+N(l-\alpha_2)_M} \\ \vdots \\ x_{(k-\beta_P)_N+N(l-\alpha_P)_M} \end{bmatrix}. \tag{11}$$

$\mathbf{X}$ can be viewed as a symbol matrix of size $P \times MN$. Let $\mathbf{X}_i$ and $\mathbf{X}_j$ be two distinct symbol matrices. The difference matrix $\mathbf{\Delta}_{ij}$ is given by $\mathbf{\Delta}_{ij} \triangleq \mathbf{X}_i - \mathbf{X}_j$. It has been shown in [6] that the asymptotic diversity order of conventional OTFS is the minimum rank of the difference matrix $\mathbf{\Delta}_{ij}, \forall i, j, i \neq j$. Let ρ_{otfs} denote the asymptotic diversity order, given by

$$\rho_{\text{otfs}} = \min_{i,j\ i\neq j} \text{rank}(\mathbf{\Delta}_{ij}). \tag{12}$$

The asymptotic diversity order for conventional OTFS has been shown to be one [6]. A lower bound on the average BER can be obtained as

$$\text{BER} \geq \frac{\kappa}{2^{MN}} \frac{1}{4\gamma MN}, \tag{13}$$

where γ is the SNR and κ denotes the number of rank one difference matrices. For ease of exposition, we assume BPSK symbols. If we were to design indexing schemes that can extract second order diversity, the task is to take a closer look at the difference matrices that contribute to diversity one and eliminate these occurrences. Towards this, we consider the following two cases.

Case 1 ($P = MN$): When $P = MN$, it is clear that the difference matrix $\mathbf{\Delta}_{ij}$ is a square matrix which is block circulant with circulant blocks. Hence, it can be diagonalized by eigen value decomposition, the eigen vectors being the columns of $\mathbf{F}_M \otimes \mathbf{F}_N$, where $\mathbf{F}_M$ and $\mathbf{F}_N$ are the Fourier matrices of order M and N, respectively. The corresponding eigen values turn out to be the MN values obtained by 2D IDFT operation on the first row vector (of size $1 \times MN$) of the difference matrix $\mathbf{\Delta}_{ij}$. For those difference matrices having rank one, there is only one non-zero eigenvalue, which implies that 2D IDFT operation results in only one non-zero value and the rest of $MN - 1$ values are zeros. For an even M and N (which is the case in practice since they are typically chosen to be the powers of 2), such rank one difference matrices can be explicitly identified and κ is found to be 8. We note that the difference matrix $\mathbf{\Delta}_{ij}$ is fully characterized by its first row. The $MN \times MN$ difference matrix can be written as

$$\mathbf{\Delta}_{ij} = \begin{bmatrix} \mathbf{\Delta}_{ij}^{(0)} & \mathbf{\Delta}_{ij}^{(1)} & \cdots & \mathbf{\Delta}_{ij}^{(M-1)} \\ \mathbf{\Delta}_{ij}^{(M-1)} & \mathbf{\Delta}_{ij}^{(0)} & \cdots & \mathbf{\Delta}_{ij}^{(M-2)} \\ \vdots & \vdots & \vdots & \vdots \\ \mathbf{\Delta}_{ij}^{(1)} & \mathbf{\Delta}_{ij}^{(2)} & \cdots & \mathbf{\Delta}_{ij}^{(0)} \end{bmatrix}, \tag{14}$$

where $\forall\ k$

$$\mathbf{\Delta}_{ij}^{(k)} = \begin{bmatrix} \delta_{ij}^{(k)(0)} & \delta_{ij}^{(k)(1)} & \cdots & \delta_{ij}^{(k)(N-1)} \\ \delta_{ij}^{(k)(N-1)} & \delta_{ij}^{(k)(0)} & \cdots & \delta_{ij}^{(k)(N-2)} \\ \vdots & \vdots & \vdots & \\ \delta_{ij}^{(k)(1)} & \cdots & \cdots & \delta_{ij}^{(k)(0)} \end{bmatrix}, \tag{15}$$

where $\delta_{ij}^{(k)(l)}$ is the lth element in the first row of the kth circulant matrix $\mathbf{\Delta}_{ij}^{(k)}$ of dimension $N \times N$. In Table I, we enumerate the first row of the 8 rank one difference matrices[1].

Case 2 ($P \neq MN$): Here, we consider a $N \times M$ channel grid with P non-zero values filled over a subgrid of size $r_1 \times r_2$ such that $P = r_1 r_2$, i.e., $\alpha_i \in \{0, 1, \cdots, r_2 - 1\}$ and $\beta_i \in \{0, 1, \cdots, r_1 - 1\}$. For such a channel structure, from (10), $\mathbf{X}$ forms a partial block circulant matrix (r_2 consecutive blocks out of M) with partial circulant blocks (r_1 consecutive rows out of N). Hence, in this case, the partial difference matrix, denoted by $\left(\mathbf{\Delta}'_{ij}\right)_{r_1 r_2 \times MN}$, also has the same structure. We now have the following theorem.

Theorem 1: $\left(\mathbf{\Delta}'_{ij}\right)_{r_1 r_2 \times MN}$ is rank one if and only if $\left(\mathbf{\Delta}_{ij}\right)_{MN \times MN}$ is rank one.

Proof: The $r_1 r_2 \times MN$ partial difference matrix can be written as

$$\mathbf{\Delta}'_{ij} = \begin{bmatrix} \mathbf{\Delta}'_{ij}{}^{(0)} & \mathbf{\Delta}'_{ij}{}^{(1)} & \cdots & \mathbf{\Delta}'_{ij}{}^{(M-1)} \\ \mathbf{\Delta}'_{ij}{}^{(M-1)} & \mathbf{\Delta}'_{ij}{}^{(0)} & \cdots & \mathbf{\Delta}'_{ij}{}^{(M-2)} \\ \vdots & \vdots & \vdots & \vdots \\ \mathbf{\Delta}'_{ij}{}^{(M-(r_2-1))} & \cdots & \cdots & \mathbf{\Delta}'_{ij}{}^{(M-r_2)} \end{bmatrix}, \tag{16}$$

where $\forall\ k$

$$\mathbf{\Delta}'_{ij}{}^{(k)} = \begin{bmatrix} \delta_{ij}^{(k)(0)} & \delta_{ij}^{(k)(1)} & \cdots & \delta_{ij}^{(k)(N-1)} \\ \delta_{ij}^{(k)(N-1)} & \delta_{ij}^{(k)(0)} & \cdots & \delta_{ij}^{(k)(N-2)} \\ \vdots & \vdots & \vdots & \\ \delta_{ij}^{(k)(N-(r_1-1))} & \cdots & \cdots & \delta_{ij}^{(k)(N-r_1)} \end{bmatrix}, \tag{17}$$

[1]If either of M or N is odd, then $\kappa = 4$ and only the first four rows of Table I are valid. If both M and N are odd, then $\kappa = 2$ and only the first two rows of Table I are valid.

Sl.No	First rows of Δ_{ij} (i.e., values of $\delta_{ij}^{(k)(l)}$, $k = 0$ to $M-1$; $l = 0$ to $N-1$)					
	$(k = 0;\ l = 0$ to $N-1)$	$(k = 1;\ l = 0$ to $N-1)$	$(k = 2;\ l = 0$ to $N-1)$	$(k = 3;\ l = 0$ to $N-1)$	$\cdots$	$(k = M-1;\ l = 0$ to $N-1)$
1	$2\ 2\ 2\ 2\ \cdots\ 2$	$2\ 2\ 2\ 2\ \cdots\ 2$	$2\ 2\ 2\ 2\ \cdots\ 2$	$2\ 2\ 2\ 2\ \cdots\ 2$	$\cdots$	$2\ 2\ 2\ 2\ \cdots\ 2$
2	$-2\ -2\ -2\ -2\ \cdots\ -2$	$-2\ -2\ -2\ -2\ \cdots\ -2$	$-2\ -2\ -2\ -2\ \cdots\ -2$	$-2\ -2\ -2\ -2\ \cdots\ -2$	$\cdots$	$-2\ -2\ -2\ -2\ \cdots\ -2$
3	$2\ 2\ 2\ 2\ \cdots\ 2$	$-2\ -2\ -2\ -2\ \cdots\ -2$	$2\ 2\ 2\ 2\ \cdots\ 2$	$-2\ -2\ -2\ -2\ \cdots\ -2$	$\cdots$	$-2\ -2\ -2\ -2\ \cdots\ -2$
4	$-2\ -2\ -2\ -2\ \cdots\ -2$	$2\ 2\ 2\ 2\ \cdots\ 2$	$-2\ -2\ -2\ -2\ \cdots\ -2$	$2\ 2\ 2\ 2\ \cdots\ 2$	$\cdots$	$2\ 2\ 2\ 2\ \cdots\ 2$
5	$2\ -2\ 2\ -2\ \cdots\ -2$	$2\ -2\ 2\ -2\ \cdots\ -2$	$2\ -2\ 2\ -2\ \cdots\ -2$	$2\ -2\ 2\ -2\ \cdots\ -2$	$\cdots$	$2\ -2\ 2\ -2\ \cdots\ -2$
6	$-2\ 2\ -2\ 2\ \cdots\ 2$	$-2\ 2\ -2\ 2\ \cdots\ 2$	$-2\ 2\ -2\ 2\ \cdots\ 2$	$-2\ 2\ -2\ 2\ \cdots\ 2$	$\cdots$	$-2\ 2\ -2\ 2\ \cdots\ 2$
7	$2\ -2\ 2\ -2\ \cdots\ -2$	$-2\ 2\ -2\ 2\ \cdots\ 2$	$2\ -2\ 2\ -2\ \cdots\ -2$	$-2\ 2\ -2\ 2\ \cdots\ 2$	$\cdots$	$-2\ 2\ -2\ 2\ \cdots\ 2$
8	$-2\ 2\ -2\ 2\ \cdots\ 2$	$2\ -2\ 2\ -2\ \cdots\ -2$	$-2\ 2\ -2\ 2\ \cdots\ 2$	$2\ -2\ 2\ -2\ \cdots\ -2$	$\cdots$	$2\ -2\ 2\ -2\ \cdots\ -2$

TABLE I
FIRST ROWS OF THE 8 RANK ONE DIFFERENCE MATRICES.

where $\delta_{ij}^{(k)(l)}$ is the lth element in the first row of the kth partial circulant matrix $\mathbf{\Delta}'^{(k)}_{ij}$, whose dimension is $r_1 \times N$. Now, let us define $\mathbf{F} = \mathbf{F}_M \otimes \mathbf{F}_N$ and its corresponding $r_1 r_2 \times MN$ partial matrix as

$$\mathbf{F}' = \begin{bmatrix} \mathbf{F}'_N & \mathbf{F}'_N & \cdots & \mathbf{F}'_N \\ \mathbf{F}'_N & \omega_M \mathbf{F}'_N & \cdots & \omega_M^{(M-1)} \mathbf{F}'_N \\ \vdots & \vdots & \ddots & \vdots \\ \mathbf{F}'_N & \omega_M^{(r_2-1)} \mathbf{F}'_N & \cdots & \omega_M^{(r_2-1)(M-1)} \mathbf{F}'_N \end{bmatrix} \tag{18}$$
$$= \mathbf{F}'_M \otimes \mathbf{F}'_N,$$

where, defining $\omega_N = e^{j\frac{2\pi}{N}}$ and $\omega_M = e^{j\frac{2\pi}{M}}$,

$$\mathbf{F}'_N = \begin{bmatrix} 1 & 1 & \cdots & 1 \\ 1 & \omega_N & \cdots & \omega_N^{(N-1)} \\ \vdots & \vdots & \ddots & \vdots \\ 1 & \omega_N^{(r_1-1)} & \cdots & \omega_N^{(r_1-1)(N-1)} \end{bmatrix}, \tag{19}$$

$$\mathbf{F}'_M = \begin{bmatrix} 1 & 1 & \cdots & 1 \\ 1 & \omega_M & \cdots & \omega_M^{(M-1)} \\ \vdots & \vdots & \ddots & \vdots \\ 1 & \omega_M^{(r_2-1)} & \cdots & \omega_M^{(r_2-1)(M-1)} \end{bmatrix}, \tag{20}$$

By the property of Kronecker product,

$$\text{rank}(\mathbf{F}') = \text{rank}(\mathbf{F}'_M).\text{rank}(\mathbf{F}'_N). \tag{21}$$

Since $\mathbf{F}'_N$ and $\mathbf{F}'_M$ are Vandermonde matrices [14], they are full rank matrices with ranks r_1 and r_2, respectively. So, the rank of $\mathbf{F}'$ is $r_1 r_2$. It can be further verified that

$$\mathbf{\Delta}'_{ij}\mathbf{F} = \mathbf{F}'\mathbf{D}, \tag{22}$$

where

$$\mathbf{D} = diag(g(1), g(\omega_M^0, \omega_N^1), g(\omega_M^0, \omega_N^2), \cdots g(\omega_M^{M-1}, \omega_N^{N-1})) \tag{23}$$

and

$$g(x_1, x_2) = \sum_{k=0}^{M-1} \sum_{l=0}^{N-1} \delta_{ij}^{(k)(l)} x_1^k x_2^l. \tag{24}$$

The values in $\mathbf{D}$ are nothing but the eigen values of $\mathbf{\Delta}_{ij}$. If $\mathbf{\Delta}'_{ij}$ is rank one, then $\mathbf{D}$ has only one non-zero value which implies $\mathbf{\Delta}_{ij}$ is also rank one. Therefore, the rank one matrices for both cases $P = MN$ and $P \neq MN$ are the same.

In order to get second order diversity, we need to eliminate these rank one cases. Applying index modulation can aid the elimination of rank one cases. Indexing introduces zeros in non active indices. By wisely choosing the number of active delay and Doppler indices, we can eliminate the rank one difference matrices from occurring in the signal set. In both 1D and 2D indexing, there are some possibilities of occurrence of rank one difference matrices in the signal set.

In all three types of 2D indexing as described in Sec. II-A, there are two cases where we obtain rank one difference matrices. These two cases occur when $i)$ $K_1 = M/2$ and $K_2 = N$, and $ii)$ $K_1 = M$ and $K_2 = N/2$. In the above two cases, symbols from the modulation alphabet fill half the bins in the $N \times M$ DD grid, and there is a possibility of occurrence of completely filled difference matrices whose first rows follow the same pattern as those in Table I with values scaled by a factor of 0.5. Except for the above mentioned K_1 and K_2 values, it can be verified that all other values of K_1 and K_2 will produce a difference matrix set with no rank one difference matrix in it. Therefore, the asymptotic diversity order achieved by OTFS with 2D indexing is two. $\square$

We will verify the above diversity result through simulations in the next section.

IV. DIVERSITY AND PAPR RESULTS

A. Diversity performance

In this subsection, the diversity performance of both 1D indexed (delay indexed and Doppler indexed) and 2D indexed OTFS systems with maximum likelihood (ML) detection are presented. The results are compared with those of conventional OTFS (without indexing). Table II shows the simulation parameters used. Figure 2 shows the BER performance of $i)$ delay indexed OTFS with $M = 4$, $N = 2$, $K_1 = 1$, and 4-QAM, and $ii)$ conventional OTFS with $M = 4$, $N = 2$, and BPSK. Both systems have 1 bpcu rate. It can be seen from the Fig. 2 that the simulated BER of the delay indexed system attains an asymptotic diversity order of two and the conventional OTFS system attains an asymptotic diversity order of one, which verifies the analytical results in Sec. III. We can also observe that delay indexed system achieves SNR gains of 1 dB and 2 dB at a BER of 10^{-3} and 10^{-4}, respectively, compared to conventional OTFS. Figure 3 shows the second order diversity performance achieved by Type 2 2D indexed OTFS system with $M = 4$, $N = 2$, $K_1 = 2$, $K_2 = 1$, 4-QAM, and 1 bpcu. The rank histogram of the difference matrices corresponding to Figs. 2 and 3 are given in Table III, where we can see that the indexed OTFS systems considered have no rank one difference matrices, and hence they attain a diversity order of two, as observed Figs. 2 and 3.

For practical large values of M and N, ML detector becomes impractical due to its exponentially growing decoding complexity. Message passing (MP) algorithms are used to attain near-optimal and low-complexity detection in such cases where M and N are large. The system model given in (6) can be modeled as a sparsely connected fac-

Parameter	Value
Carrier frequency (GHz)	4
Subcarrier spacing (KHz)	3.75
Number of paths (P)	4
Delay-Doppler profile (τ_i, ν_i)	$(0,0), (0, \frac{1}{NT}),$ $(\frac{1}{M\Delta f}, 0), (\frac{1}{M\Delta f}, \frac{1}{NT})$

TABLE II
SIMULATION PARAMETERS (FOR FIGURES 2 & 3).

System	Ranks			
	1	2	3	4
$M = 4,\ N = 2$ w/o indexing	8	2328	1536	61408
$M = 4,\ N = 2,\ K_1 = 1$ 1D delay indexing	0	1056	512	63712
$M = 4,\ N = 2,\ K_1 = 2,\ K_2 = 1$ 2D Type 2 indexing	0	1664	768	62848

TABLE III
RANK HISTOGRAM OF DIFFERENCE MATRICES.

tor graph. Scalar messages are exchanged between MN variable nodes and MN observation nodes to get an estimate of the transmitted symbols in the message passing based detection [5]. In MP detector for indexed systems, an additional layer of DD bin activation pattern nodes are used to exploit the structure obtained from indexing [16]. A carrier frequency of 4 GHz, subcarrier spacing of 15 KHz, number of paths $P = 6$, and a DD profile (τ_i, ν_i) = $\{(0,0),\ (0, \frac{1}{NT}),\ (\frac{1}{M\Delta f}, 0),\ (\frac{1}{M\Delta f},\ \frac{1}{NT}),\ (\frac{2}{M\Delta f}, 0),\ (\frac{2}{M\Delta f}, \frac{1}{NT})\}$ are used for simulations. Figure 4 shows the BER performance of $i)$ 1D delay indexed OTFS with $M = 8$, $N = 8$, $K_1 = 2$, and 4-QAM, and $ii)$ conventional OTFS with $M = 8$, $N = 8$, and BPSK, each having 1 bpcu rate. We can observe that 1D delay indexed OTFS performs better than conventional OTFS, which is attributed to the higher diversity order achieved by the proposed indexing in OTFS.

B. PAPR performance

In this subsection, the PAPR performance of 1D indexed OTFS system is analyzed. As discussed in Sec. II, the information symbols mounted on DD grid are transformed to time domain using ISFFT followed by Heisenberg transform. Let $\mathbf{X}$ denote the $N \times M$ matrix containing the information symbols in the DD grid. The ISFFT operation can be viewed as N-point IDFT along the columns and M-point DFT along the rows of $\mathbf{X}$. Assuming rectangular transmit and receive pulses, the OTFS transmit signal in matrix form is given by

$$\mathbf{S} = \mathbf{F}_N^H \mathbf{X} \mathbf{F}_M \mathbf{F}_M^H = \mathbf{F}_N^H \mathbf{X}, \tag{25}$$

where $\mathbf{F}_N$ and $\mathbf{F}_M$ are the N-point and M-point DFT matrices, respectively. It can be observed from (25) that the N-point IDFT is performed along the columns of $\mathbf{X}$ which makes the maximum PAPR of OTFS modulation vary linearly with N and not with M [15].

In 1D indexing along the Doppler axis, there will be only K_2 active bins along the columns of $\mathbf{X}$. So, the maximum PAPR of 1D indexing along the Doppler axis depends on the value of $K_2 < N$. The maximum PAPR in this indexing scheme will be $\text{PAPR}_{\text{max}} = K_2 \text{PAPR}_{\text{c}}$, where PAPR_{c} is the PAPR of the modulation alphabet used. In 1D indexing along the delay axis, there can be up to N active bins along the

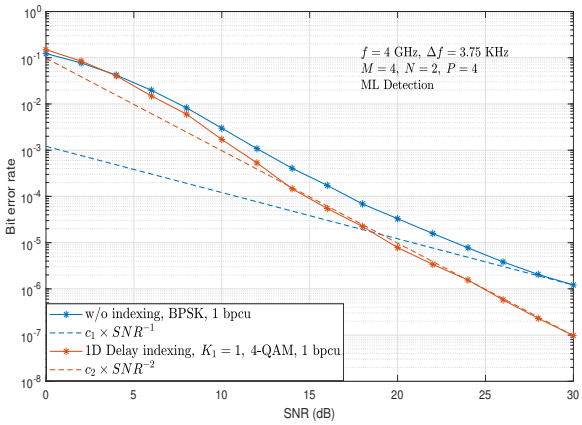

Fig. 2. BER performance of 1D delay indexed OTFS and conventional OTFS (without indexing) using ML detection.

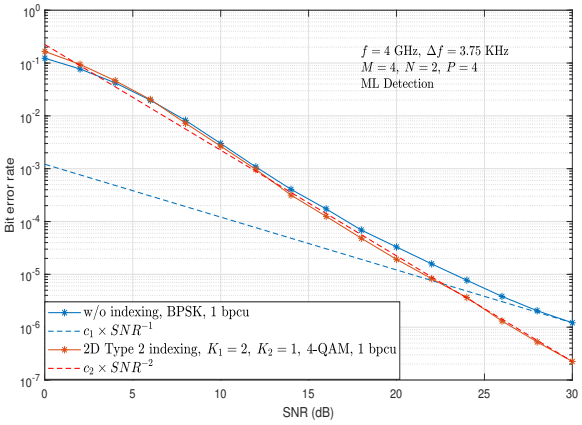

Fig. 3. BER performance of 2D Type 2 indexed OTFS and conventional OTFS (without indexing) using ML detection.

columns of $\mathbf{X}$. Since the average power transmitted in this delay indexed scheme is lower compared to conventional OTFS scheme, the maximum PAPR of 1D indexing along the delay axis will be $\text{PAPR}_{\text{max}} = (NM/K_1)\text{PAPR}_{\text{c}}$.

Figure 5 shows the CCDF of PAPR of delay indexed and Doppler indexed OTFS systems with $M = 32$, $N = 32$, $K_1 = 16$ and $K_2 = 16$, and conventional OTFS system with $M = 32$ and $N = 32$. All systems use 4-QAM and Nyquist sampling (oversampling ratio = 1). It can be seen from the figure that the PAPR performance of the Doppler indexed OTFS system is better than the conventional OTFS system. Since $K_2 < N$, the maximum PAPR value of Doppler indexed system is lower compared to conventional OTFS system. From the figure, we can observe that the delay indexed OTFS system has higher PAPR compared to conventional OTFS system. This is because the PAPR_{max} value of the delay indexed OTFS system is higher compared to conventional OTFS system.

Effect of number of active bins : Figure 6 shows the CCDF of PAPR of delay indexed and Doppler indexed OTFS systems with $M = 32$, $N = 32$, $K_1 = 12, 16$, and $K_2 = 12, 16$. Both systems use 4-QAM and Nyquist sampling (oversampling ratio = 1). From Fig. 6, we can observe that the Doppler indexed

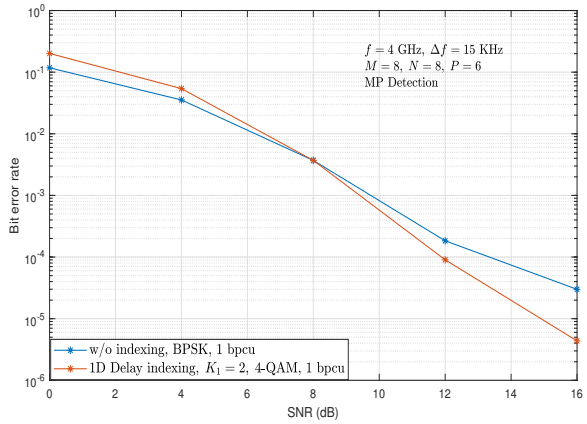

Fig. 4. BER performance of 1D delay indexed OTFS and conventional OTFS (without indexing) using message passing detection.

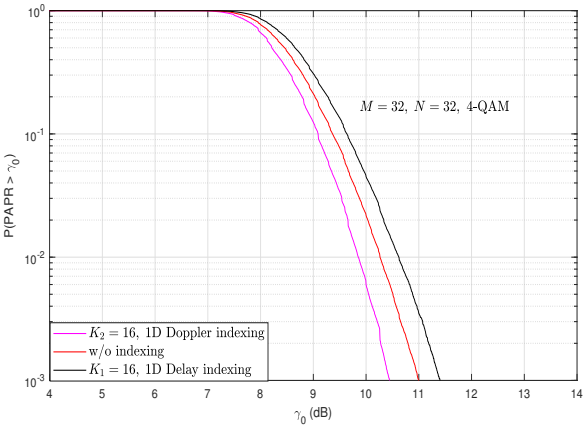

Fig. 5. Comparison of CCDF of PAPR of Doppler indexed, delay indexed, and conventional OTFS systems.

system with smaller number of active bins (K_2) have lower PAPR values. It can be seen that the PAPR_{max} value of Doppler indexed system linearly varies with K_2. In contrast, the delay indexed system with smaller number of active bins (K_1) has higher PAPR values. It can be seen that the PAPR_{max} of delay indexed system has an inverse dependence on the value of K_1.

V. Conclusions

We proposed DD indexing designs for OTFS that can achieve an asymptotic diversity order of two. This is an interesting new contribution given that the asymptotic diversity order of conventional OTFS (without indexing) is just one. We achieved this diversity order of two by eliminating the occurrences of rank one difference matrices. Simulation results validated the analytically proved second order diversity. We also showed that DD indexing can improve the PAPR performance of OTFS. The effect of pulse shapes on the diversity performance of indexed OTFS is a topic of future work. Also, DD indexing designs to achieve more than diversity order two can be investigated as future work.

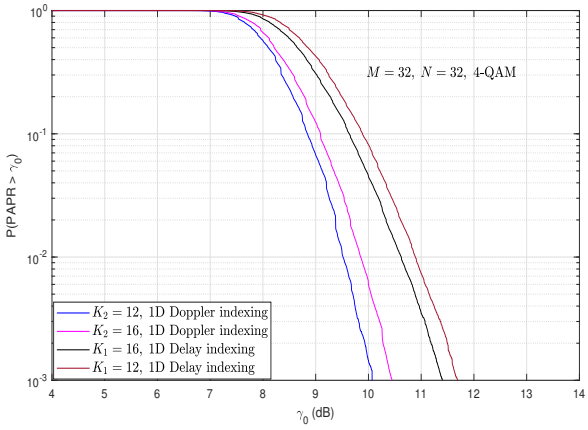

Fig. 6. Effect of active bins on the CCDF of PAPR of delay indexed and Doppler indexed OTFS systems.

References

[1] R. Hadani, S. Rakib, M. Tsatsanis, A. Monk, A. J. Goldsmith, A. F. Molisch, and R. Calderbank "Orthogonal time frequency space modulation," in *Proc. IEEE WCNC'2017*, Mar. 2017, pp. 1-6.

[2] R. Hadani and A. Monk, "OTFS: a new generation of modulation addressing the challenges of 5G," available [online]: https://arxiv.org/abs/1802.02623, Feb. 2018.

[3] R. Hadani, S. Rakib, S. Kons, M. Tsatsanis, A. Monk, C. Ibars, J. Delfeld, Y. Hebron, A. J. Goldsmith, A.F. Molisch, and R. Calderbank "Orthogonal time frequency space modulation," available [online]: https://arxiv.org/abs/1808.00519v1, Aug. 2018.

[4] S. K. Mohammed, "Derivation of OTFS modulation from first principles," available [online]: https://arxiv.org/abs/2007.14357, Jul. 2020.

[5] P. Raviteja, K. T. Phan, Y. Hong, and E. Viterbo, "Interference cancellation and iterative detection for orthogonal time frequency space modulation," *IEEE Trans. Wireless Commun.*, vol. 17, no. 10, pp. 6501-6515, Oct. 2018.

[6] G. D. Surabhi, R. M. Augustine, and A. Chockalingam, "On the diversity of uncoded OTFS modulation in doubly-dispersive channels," *IEEE Trans. Wireless Commun.*, vol. 18, no. 6, pp. 3049-3063, Jun. 2019.

[7] A. Nimr, M. Chafii, M. Matthe, and G. Fettweis, "Extended GFDM framework: OTFS and GFDM comparison," in *Proc. IEEE GLOBECOM'2018*, Dec. 2018.

[8] P. Raviteja, E. Viterbo, and Y. Hong, "OTFS performance on static multipath channels," *IEEE Wireless Commun. Lett.*, vol. 8, no. 3, pp. 745-748, Jun. 2019.

[9] J. Zhang, A. D. S. Jayalath, and Y. Chen, "Asymmetric OFDM systems based on layered FFT structure," *IEEE Signal Process. Lett.*, vol. 14, no. 11, pp. 812-815, Nov. 2007.

[10] E. Basar, "Index modulation techniques for 5G wireless networks," *IEEE Commun. Mag.*, pp. 168-175, Jul. 2016.

[11] E. Basar, M. Wen, R. Mesleh, M. Di Renzo, Y. Xiao and H. Haas, "Index modulation techniques for next-generation wireless networks," *IEEE Access*, vol. 5, pp. 16693-16746, 2017.

[12] B. Shamasundar, S. Jacob, S. Bhat, and A. Chockalingam, "Multidimensional index modulation in wireless communications," *IEEE Access*, vol. 6, pp. 589-604, 2018.

[13] Y. Liang, L. Li, P. Fan, and Y. Guan, "Doppler resilient orthogonal time-frequency space (OTFS) systems based on index modulation," *IEEE VTC2020-Spring*, May 2020, pp. 1-5.

[14] Y. Fan, H. Liu, "Double circulant matrices," available [online]: https://arxiv.org/abs/1601.06872v1, Jan. 2016.

[15] G. D. Surabhi, R. M. Augustine, and A. Chockalingam, "Peak-to-average power ratio of OTFS modulation," *IEEE Commun. Lett.*, vol. 23, no. 6, pp. 999-1002, Jun. 2019.

[16] Y. Niu and J. Zheng, "Message passing algorithm for GFDM-IM detection," *IEEE Intl. Conf. on DSP*, 2018, pp. 1-5.